IEICE Proceeding Series

Inferring interdependencies in climate networks constructed at inter-annual, intra-season and longer time scales

J. Ignacio Deza, Marcelo Barreiro, Cristina Masoller

Vol. 1 pp. 235-238
Publication Date: 2014/03/17
Online ISSN: 2188-5079

2012 International Symposium on Nonlinear Theory and its Applications
NOLTA2012, Palma, Majorca, Spain, October 22-26, 2012

Inferring interdependencies in climate networks constructed at inter-annual, intra-season and longer time scales

J. Ignacio Deza†, Marcelo Barreiro‡ and Cristina Masoller†

†Departament de Física i Enginyeria Nuclear, Universitat Politecnica de Catalunya,
Colom 11. E-08222, Terrassa, Barcelona, Spain.
‡Instituto de Física, Facultad de Ciencias, Universidad de la Repblica,
Iguá, 4225, Montevideo, Uruguay.
Emails: juan.ignacio.deza@upc.edu, cristina.masoller@upc.edu

Abstract—We study global climate networks constructed at various time-scales by means of ordinal time series analysis of monthly-averaged surface air temperature (SAT) anomalies. To quantify climate interdependencies, we compute the mutual information from the anomaly values and from its symbolic, ordinal-based representation. The ordinal analysis allows to identify changes in the topology of the network when varying the pattern, covering a short, intra-season time scale (e.g., of a few months) to a longer, inter-annual time scale (e.g., of a few years). We report changes in the network topology with the various time-scales and present evidence of correlations between geographical regions that occur at certain time scales only.

1. Introduction

Complex networks appear in almost all fields of science, examples being the internet, social interactions, food webs, biochemical reactions, brain functional networks, etc. For the purpose of modeling and forecasting, many systems lead naturally to the concept of networks of interacting elements, where one can define nodes and assign links among them depending on the (in principle, very complex) features of the system under study. Using the network approach is then possible to extract relevant information about a system without over simplifying it or without having to handle the full scale detailed model which can obscure the interpretations. This is precisely the situation in the field of climate networks.

Since the atmosphere connects geographically far away regions through waves and advection of heat and momentum, this long-range coupling makes the network modeling approach of the Earth's climate extremely attractive and promising [1]. By covering the Earth' surface with a regular grid of nodes, and by assigning links to connections between two different nodes via an analysis of their climate interdependency, the network approach has been shown to be able to extract novel and meaningful information [2, 3, 4].

Recently, two of us studied the Earth climate network employing methods of nonlinear time-series analysis [5]; specifically, ordinal patterns and symbolic binary representations of the monthly-averaged surface air temperature (SAT) anomalies. A main advantage of this symbolic methodology is that, by varying the length of time-period in the ordinal or binary pattern, the analysis uncovered memory processes with different time scales, that result in climate networks with different structures. Here we analyze how the network structure varies when varying the length of the pattern and also compare with the climate network obtained directly from SAT anomalies, i.e., without applying the symbolic transformation.

2. Network construction

We analyze the monthly-averaged SAT anomalies (reanalysis data of the National Center for Environmental Prediction/National Center for Atmospheric Research, NCEP/NCAR). The anomalies are calculated as the actual temperature values minus their monthly average, and are normalized to the standard deviation. The data covers a uniform grid over the Earth's surface with latitudinal and longitudinal resolution of 2.5°, resulting in 10226 grid points or network nodes. In each node the data covers the period from January 1949 to December 2006, which gives 696 months or data points.

The climate network properties will depend on the methodology employed to infer the presence of connections between two network nodes, i.e., the procedure used to include a particular link in the network and to filter out those correlations that may have occurred merely by chance.

As in Refs. [1, 5], to quantify climate interdependencies we use the Mutual information (MI), that is a nonlinear symmetric measure; is a function of the probability density functions (PDFs) that characterize the time series in two nodes, $p_i(m)$ and $p_j(n)$, as

well as of their joint probability $p_{ij}(m,n)$.

$$M_{ij} = \sum_{m,n} p_{ij}(m,n) \log \frac{p_{ij}(m,n)}{p_i(m)p_j(n)}. \qquad (1)$$

M_{ij} measures the degree of statistical interdependency as, if the two time series independent, $p_{ij}(m,n) = p_i(m)p_j(n)$ and thus, $M_{ij} = 0$.

The MI was calculated from Eq. (1) with different PDFs associated to the time series: one being the usual histogram of values (we refer to this as MIH), and the other being the histogram of symbolic patterns, referred to as ordinal patterns (OPs) [6].

The OPs are calculated from the time series by noting the value of a given point relative to its neighboring points in the series. For instance, for patterns of length 3, if a value (v_2) is higher than the previous one (v_1) but lower than the next one (v_3), gives the pattern '123', while the opposite case ($v_1 > v_2 > v_3$) gives the pattern '321'. This allows to detect correlations in the time series (which are not taken into account with histograms of values), but has the drawback that does not provide information on the relative values (if v_1 is twice v_2 or only slightly bigger, the pattern will be the same).

Ordinal patterns do not constrain us to construct the pattern with immediately adjacent points. We can construct them allowing a time interval between points, and in this way we can consider different time scales.

In this paper we consider patterns of length 4 and calculated the MI, Eq. (1), with the PDFs given by the probabilities of OPs formed by:

- four consecutive months (i.e., by comparing four consecutive points in the time series), we refer to the MI computed in this way as MI01;

- four months in consecutive seasons covering one-year period (i.e., by comparing v_i, v_{i+3}, v_{i+7} and v_{i+11}), we refer to this as MI03

- four months in consecutive years (i.e., by comparing v_i, v_{i+12}, v_{i+24} and v_{i+36}), we refer to this as MI12.

The next step is to filter the non-significant links, those between pairs of nodes i and j such that their M_{ij} value is consistent with that of a random value. The detection of weak but significant links is a challenging task that is nowadays being the subject of intensive research (see, e.g., Ref. [7]).

Here we use the simplest approach by employing surrogated time series: we calculated the M^s_{ij} values (with the supra-indice s representing surrogated data) and found they are Gaussian-like distributed (see Fig. 1), both, when the PDFs in Eq. (1) are computed from histograms of values of surrogated data and also when they are computed from histograms of OPs constructed from surrogated data. Therefore, we computed the mean value, μ, and standard deviation, σ, of the M^s_{ij} distribution and decided to accept links as significant, if they are either above $\mu + 3.4\sigma$ or below $\mu - 3.4\sigma$. This criterium gives 99.999% of confidence that the accepted links have MI values that could not be due to chance.

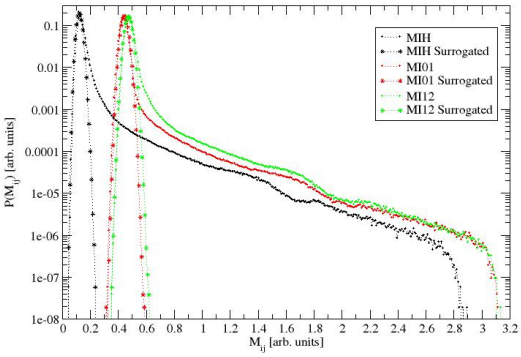

Figure 1: Probability distribution function of MI values computed from SAT anomalies and their ordinal pattern representations, for original and surrogated data.

The final step is to represent the climate network. This is done by plotting the number of links every node has, taking into account that the nodes represent geographic regions with different area (points near the poles representing a smaller area than points near the equator) and thus we represent the *area-weighted connectivity* (AWC) [1, 3, 5], which is the fraction of the total area of the Earth to which a node i is connected,

$$AWC_i = \frac{\sum_j^N A_{ij} \cos(\lambda_i)}{\sum_j^N \cos(\lambda_j)}, \qquad (2)$$

where λ_i is the latitude of node i and $A_{ij} = 1$ if nodes i and j are connected and zero otherwise. The cosine term corrects the factors relative to the planar projection of a spherical earth. Note that the AWC plots provide information about the size of the total area to which a node is connected, but do not indicate to which node a node is connected.

3. Results and discussion

In Fig. 2 we present the results of the four network construction methods. Figure 2(a) displays the network constructed with the MIH climate interdependency quantifier; Fig 2(b), with MI01; Fig 2(c), with MI03 and Fig. 2(d), with MI12.

In Fig 2(a) one can observe highly connected spots which are present only in some of the other three maps. See, for example, the high connected green spot in the Labrador Sea in Fig. 2(a), which is also

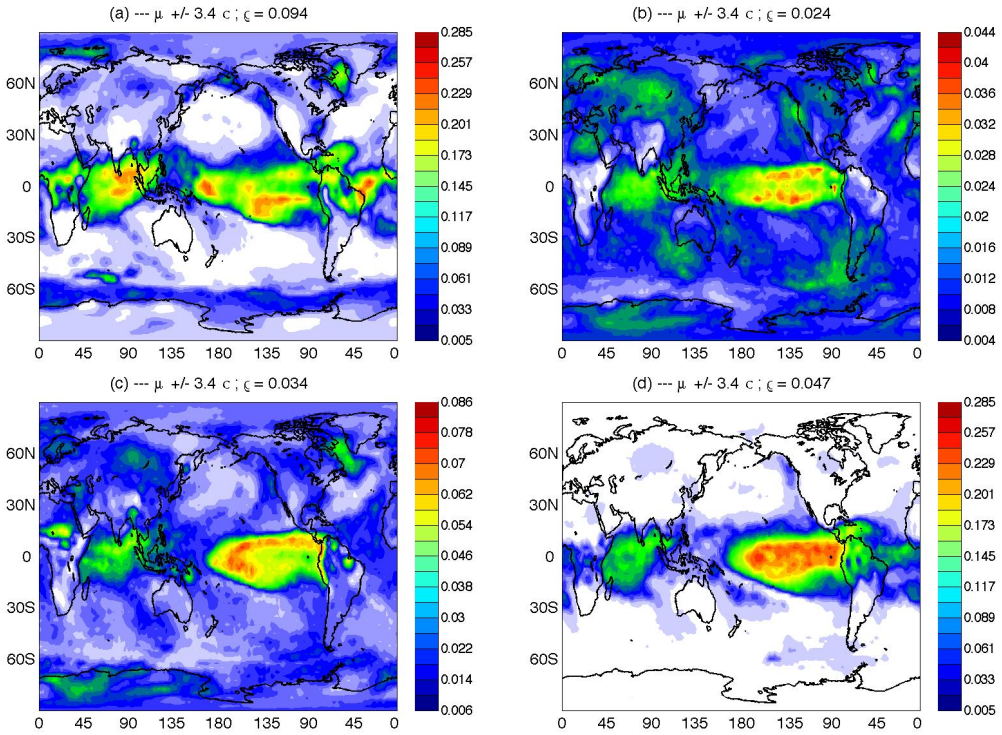

Figure 2: AWC for the different methods of network construction. (a) MI from histogram of time series, (b) MI from monthly OP, (c) MI from OP taken every three months and (d) MI from yearly OP. It can be seen that the "hub area" is localized geographically in the equatorial zone, especially it the pacific area. The title of each plot indicates the density of links, ζ, and the significance threshold used ($\mu \pm 3.4\sigma$, where μ and σ are the mean and the standard deviation of the distribution of M^s_{ij} values computed from surrogated data, shown in Fig. 1). In Figs. 2 (b), (c) and (d) one can observe that the pacific equatorial area grows in importance as the ordinal pattern takes in account longer time-scales. Note how some structures present in (a) are found in some of the other maps, suggesting that those links are tuned to a particular time scale.

seen in Fig. 2(c) and to a lesser extent in Fig 2 (b), but is not present in Fig. 2(d). Also, one can notice in Fig. 2(a) highly connected areas in Africa, the equatorial Atlantic and western tropical north Atlantic which are not present in the short-time scale networks, Figs. 2(b), (c), but that are seen in the year-time scale network, Fig. 2(d). Thus, these regions are connected on inter-annual, but not on monthly or seasonal time scales. The western tropical north Atlantic is known to warm due to atmospheric circulation anomalies caused by El Nino-Southern Oscillation (ENSO) [8]. The equatorial Atlantic is also influenced by ENSO but could also force by itself temperature anomalies in neighboring regions. Therefore, the OP symbolic method allows to see how the network topology is modified by climate processes acting on different time scales.

In Fig. 2 one can also observe that the networks constructed with MI01 and MI03 are more homogenously connected than those constructed with MIH and MI12, even though the tropical Pacific still stands out. This suggests that on short time scales there is no dominant phenomenon that interconnects remote regions. Instead, temperature anomalies seem to be governed by regional patterns of atmospheric internal variability.

In spite of the fact that we have used the same significance criterium for the four networks, the number of links are significantly different, due to the fact that the values of M_{ij} have a distribution with different mean and shape, depending on how the PDFs are calculated (see Fig. 1). An alternative approach would be to vary the significance threshold and to adjust the threshold such that the four networks have a similar number of links. This approach was used in [5] where it was also found that the short-time scale network MI01 was more uniformly connected than MI12.

Acknowledgments

The research was funded by the European Community's Seventh Framework Programme under grant agreement 289447 (climatelinc.eu).

References

[1] J. F. Donges, Y. Zou, N. Marwan and J. Kurths, *Eur. Phys. J. Spec. Top.*, Vol. 174, pp. 157, (2009).

[2] K. Yamasaki, A. Gozolchiani and S. Halvin, Phys. Rev. Lett. **100**, 228501 (2008).

[3] A. A. Tsonis and K. L. Swanson, Phys. Rev. Lett. **100**, 228502 (2008).

[4] J. F. Donges, Y. Zou, N. Marwan et al., EPL **87** 48007 (2009).

[5] M. Barreiro, A. C. Marti and C. Masoller. *Chaos*, Vol. 21 013101 (2011).

[6] C. Bandt and B. Pompe, Phys. Rev. Lett. **88**, 174102 (2002).

[7] M. Palus, D. Hartman, J. Hlinka, and M. Vejmelka, Nonlin. Processes Geophys. 18, 751 (2011).

[8] M. Barreiro, P. Chang, L. Ji, R. Saravanan, and A. Giannini, Dynam. Atmos. Oceans, Special Issue on Coupled tropical ocean-atmosphere dynamics and predictability, 39 (2005).